Proceedings of the ASME Internal Combustion Engine Division 2009 Spring Technical Conference
ICES2009
May 3-6, 2009, Milwaukee, Wisconsin, USA

ICES2009-76080

UNDERSTANDING THE FUNDAMENTALS OF PISTON RING AXIAL MOTION AND TWIST AND THE EFFECTS ON BLOW-BY

Richard Mittler and Albin Mierbach
Technology Rings & Liners, Federal-Mogul Corporation
Federal Mogul Burscheid GmbH
richard.mittler@federalmogul.com

Dan Richardson, Ph.D
Cummins, Inc.

ABSTRACT

Advances in modern engine development are becoming more and more challenging. The intense increase of thermal and mechanical loads interacting in the combustion chamber as a result of higher power density requires perfecting the function of piston rings especially with regard to emission reduction technology.
The major obstacle to predicting blow-by and oil consumption is the behavior of the piston rings under engine operating conditions. Design and functionality of a piston ring are highly influenced by the operating conditions. To understand the fundamentals of ring behavior and in this way the effects on blow-by and oil consumption, an analytical tool has been developed to transform the physical boundary conditions of engine kinematics and ring design into a reliable simulation. This paper describes the physical basics of ring movement under dynamic loading conditions and gives an overview of the results. It also was necessary to validate the model with real engine measurements to understand the fundamentals of ring design as a function of the described mathematics.

INTRODUCTION

Piston rings in engines achieve efficient sealing with both the cylinder wall in a radial direction and the top or bottom sides of the piston ring grooves in an axial direction. The contact pressure on the cylinder wall is achieved by the inherent spring force of the ring in conjunction with the gas pressure behind the ring. The contact on the side of the piston groove is achieved by the axial forces acting on the ring. The axial forces are composed of the gas pressure above and under the ring, the mass forces (inertia), and the friction forces. These forces change their direction during the cycle. As a result, the piston ring moves from one side of the groove to the other during the cycle.

Gas and friction forces not only create axial forces but also moments based on the piston ring center of mass. The motion of the ring starts when the resulting axial forces change directions and can no longer overcome the moments acting on the ring. In the same way the ring motion ends when the resulting axial force becomes high enough to overcome the moments acting on the ring sufficiently to force the position of the piston ring to the opposite side. Hence the change of position of a piston ring is not a sudden effect, but more a process which can possibly last 60 degrees of crank angle or more. There are also movements where the change of position starts, but full contact on the

opposite side of the groove can not be achieved. In these cases the piston ring can no longer create a seal against the ring groove flank and the combustion gas can pass around the back of the piston ring (this can occur both on the bottom side and top side). This has a significant effect on blow-by.

PART 1: INTRODUCTION MODEL

A simplified model is used to explain the mathematical relationship for the stabilized flank contact and therewith the fundamentals of the piston ring position change. In addition the simplified model is used to explain the influence of moments on the piston ring axial motion. It also describes the mathematical way of deriving a criterion for the stabilized flank contact.

The simplified model is illustrated in Figure 1. In detail forces and moments are presented in the next sections (equations 30a, 30b).

Simplifications [1]:
a) A rectangular ring is used.

b) The pressure function above and under the ring is linear.

c) In comparison to the gas pressure, friction forces are negligible.

With this simplification the fundamentals of ring movement are easily explained. It is also shown that a ring has to twist and arch during the change of position as it is influenced by moments and reaction forces.

Figure 1 shows the piston ring position on the bottom side of the ring groove with the gas pressure p_b and the volume Vol_b behind the ring.
p_b depends on the gas flow in and out through the clearances between the piston ring groove and the ring.

[1] These simplifications are only used in this section and not assumed for the whole paper. The subsequent sections are based on the realistic physical conditions.

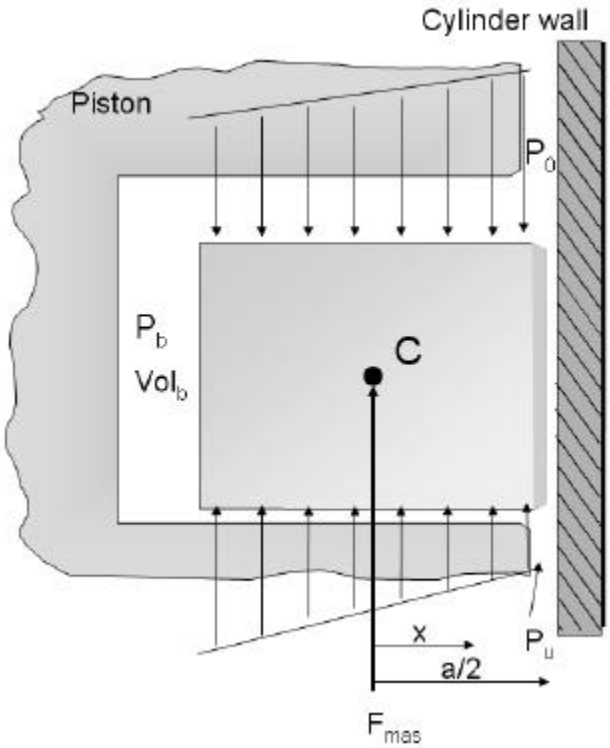

Figure 1: Typical gas pressure on the flanks of the piston ring during the cycle

The next section describes that the resulting axial gas force and the resulting gas moment are independent of the pressure p_b behind the ring. A linear formulation for the pressure in the top clearance is used:

Where:
The forces are positive in an upward direction.

$$p(x) = -\frac{1}{2}(p_o + p_b) - \frac{x}{a}(p_o - p_b) \tag{1}$$

At the bottom clearance:

$$p(x) = +\frac{1}{2}(p_u + p_b) + \frac{x}{a}(p_u - p_b) \tag{2}$$

The resulting gas pressure $p_r(x)$ is calculated with the sum of (1) and (2), if the abbreviation $\Delta p = p_o - p_u$ is implemented.

$$p_r(x) = -\frac{1}{2}\Delta p - \frac{x}{a}\Delta p \tag{3}$$

The axial gas force and the gas moment acting on the ring are calculated from equation (3) as shown below. Both values are based on the circumferential length.

$$F_{gas} = \int_{-a/2}^{a/2} p_r(x)\,dx$$

$$F_{gas} = -\frac{1}{2}\,a\,\Delta p$$

$$M_{gas} = \int_{-a/2}^{a/2} p_r(x)\,x\,dx \qquad (4\text{ a, b})$$

$$M_{gas} = -\frac{1}{12}\,a^2\Delta p$$

The resulting axial force is comprised of the mass force and the gas force. The resulting moment is equal to the gas moment because the mass force causes no moment at the center of mass.

$$F = F_{mas} - \frac{1}{2}\,a\,\Delta p$$

$$M = M_{gas} = -\frac{1}{12}\,a^2\Delta p \qquad (5\text{ a, b})$$

To reach a balance a force $F_{contact}$ is needed. $F_{contact}$ acts at the bottom flank of the groove and its point of contact has the distance h from the center of mass. The aim of this calculation is to determine the lever arm h.

.

$$F_{contact} = -F = -\left(F_{mas} + F_{gas}\right) \qquad (5\text{ c})$$

The Moment of $F_{contact}$ with the lever arm h is:

$$M_{contact} = -\left(F_{mas} + F_{gas}\right)h \qquad (5\text{ d})$$

To reach the balance of moments:

$$M_{contact} = -M$$

$$-M = -\left(F_{mas} + F_{gas}\right)h \quad \text{or}$$

$$\left(F_{mas} - \frac{1}{2}\Delta p\,a\right)h = M \qquad (6)$$

$$M = -\frac{1}{12}\Delta p\,a^2$$

$$h = \frac{-\frac{1}{12}\Delta p\,a^2}{F_{mas} - \frac{1}{2}\Delta p\,a} \qquad (7)$$

If this lever arm mathematically extends beyond the outer dimensions of the piston ring, then a contact on one piston groove side is not possible. For the balance of the forces and moments, a contact on both sides of the ring is necessary.

The new criterion for the stability contact on one groove side is:

$$-\frac{a}{2} \le h \le \frac{a}{2} \qquad (8)$$

(7) and (8) result in:

$$F_{mas} \le \frac{1}{3}\Delta p\,a \quad \text{or}$$

$$F_{mas} \ge \frac{2}{3}\Delta p\,a \qquad (9\text{ a, b})$$

The point when the gas forces (Fgas) are equivalent to the inertial forces on the ring is:

$$F_{mas} = \frac{1}{2}\Delta p\,a \qquad (10)$$

In some models, it is slightly after this point that is considered the time when the piston ring will start to move as the inertial forces start to become greater than the gas forces. However equations 9a,b show that the ring will actually start to move prior to this condition. This is illustrated in Figure 2:

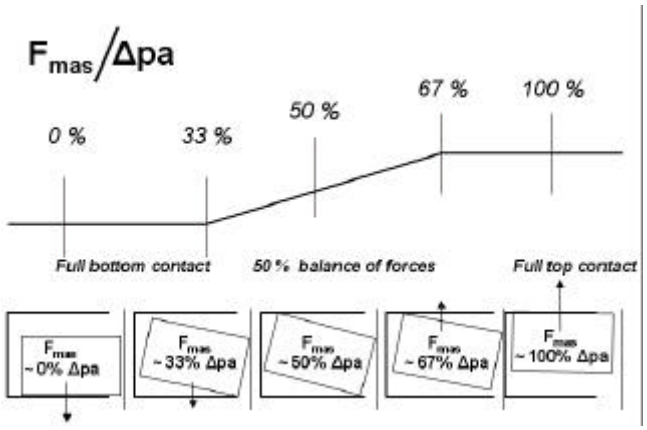

Figure 2: The change of flank contact depending on the relationship of mass force to gas force.

a) At (Fmas/Δpa) = 0% the ring has full contact on the bottom flank of the groove. Up to the ratio (Fmas/Δpa) of 33 % the supporting force at the bottom flank balances the gas moment. During this interval, the back of the ring may be slowly lifting. At 33% the piston ring only rests with the outside edge on the groove flank.

b) In excess of 33 % the ring can no longer support the gas moment with just the supporting force on the bottom side of the groove. The lever arm of the moment is outside the ring. This leads to a twist of the piston ring so that the ring is now is in contact on both the bottom and top sides of the ring groove.

c) At 50% the axial gas forces are equivalent to the inertial forces. At this point, it might be thought that the ring should start moving up to the top side of the ring groove. However as noted above, the ring had already begun its transition earlier and was actually in contact with the upper side of the groove just after 33%.

d) From 67 % and higher, the mass force becomes big enough to keep the ring totally at the top side of the groove and the ring may be resting exclusively on the top side of the ring groove.

The above description is a simple two dimensional model. In reality the full three dimensional is much more complex as described in the subsequent sessions. In this paper and in the work done by Liu et al. [13] and other, it has been found that the transition of the ring from the bottom side of the ring groove to the top side is not uniform circumferentially around the ring. The inertial forces and moments react significantly different at the ring near the end gap than 180° from the gap. As a result it is common for the ring to lift near the end gaps first.
In the condition where the ring lifts near the end gap, then the ring can no longer effectively seal the gases. The gases will vent around the ring in the raised portion. This will certainly affect blow-by.

PART 2: DETAILED MATHEMATICAL DERVIATION OF THE THEORY

Deformation of the Piston Ring through Forces and Moments

By closing a piston ring from its free shape condition to its closed condition radial bending occurs. For piston rings with non-rectangular cross sections the principal axis of inertia are not perpendicular to the cylinder axis (Figure 3). A piston ring with a non-rectangular cross section changes position by twisting and arching in axial direction [9,10]. The reason for this is that such a ring avoids the bending stress as much as possible. But a ring with a symmetrical cross section can also twist and arch if it is loaded by forces and moments. This can occur as well if the forces and the moments are constant on the circumference.

The kinematics of torsion and the bending of a curved beam were first developed by A.E.H. Love [2]. A specialized description for a circular beam can be found in Federhofer [3].

The following sections will show the calculation and analysis of bending and torsion based on this work. The methodology is described by a variation of elastic energies characterized by differential equations in conjunction with the boundary and equilibrium conditions. These equations have to be integrated under consideration of the reaction forces. The reaction forces result in response to the twist and arch of the piston ring in the groove.

It should be noted that this paper does not describe the radial forces acting on the ring including the hydrodynamic lubrication of the ring face (Reynolds equation and the Reynolds boundary condition). The details of these forces have been described in other papers. However, while the description of these forces has not been included in the subsequent sections, they are important forces that act on the ring and affect the motion and twist of the ring. These have been included in the overall model that was used.

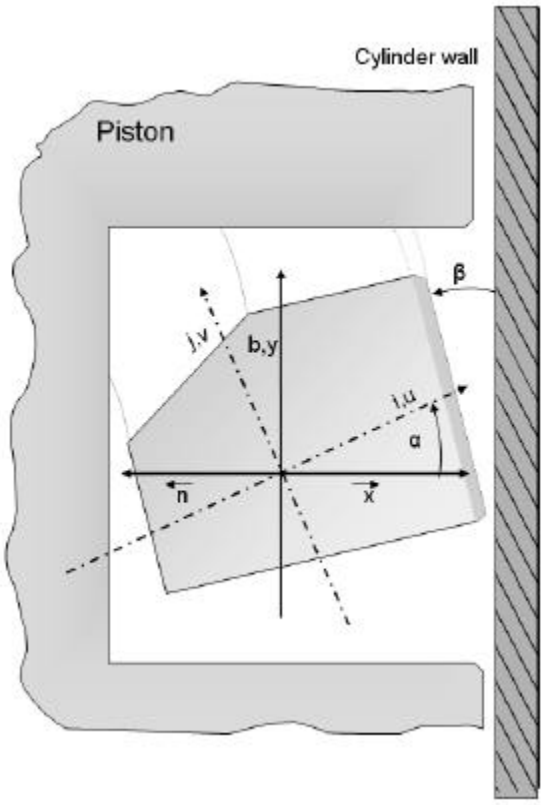

Figure 3: The main axis

Change of Curvature and Torsion

The coordinate system $(\vec{i}, \vec{j})$ of the principal axis of inertia is useful for the calculation of the elastic energy of a twisted piston ring. (Figure 3) The coordinate system $(\vec{i}, \vec{j})$ with the coordinates (u, v) is rotated by the angle α against the coordinate system (x, y).

The curvature components of the ring in the coordinate system $(\vec{i}, \vec{j})$ are:

$$\kappa_i = \frac{\sin\alpha}{r_s}$$

$$\kappa_j = \frac{\cos\alpha}{r_s} \qquad (11\ a,b)$$

Where:

r_S is the distance from the center of mass to the cylinder center axis.

The piston ring can only move to the axial direction (y). Then the movement can be resolved into u and v which are the displacement in direction of the principal axis of inertia. According to Figure 3:

$$u\cos\alpha = v\sin\alpha \qquad (12)$$

The equations (13a,b,c) are found in Federhofer [3].

$$\Delta\kappa_i = -\beta\,\kappa_j - \frac{d^2v}{ds^2} \qquad (13a)$$

$$\Delta\kappa_j = +\beta\,\kappa_i + \frac{d^2u}{ds^2} \qquad (13b)$$

$$\tau = \frac{d\left(-\beta + \kappa_i u + \kappa_j v\right)}{ds} \qquad (13c)$$

Where:

ß is the twist angle

$\Delta\kappa$ is the change of the curvatures

τ is the torsion

ds is the arc length

$$ds = r_s\,d\varphi \qquad (14)$$

Where:

φ is the ring angle $\qquad \varphi \in [-\pi, \pi]$

The acronym z will be used. z is a non-dimensional variable, which describes the displacement depending on r_S in direction of the cylinder axis.

$$z = \frac{v}{r_s\cos\alpha} \qquad (15)$$

With the equations (11, 12, 14, 15) it is possible to rewrite equation (13a,b,c). The notation used is: $\frac{df}{d\varphi} = f'$

$$r_s\,\Delta\kappa_i = -(\beta + z'')\cos\alpha \qquad (16a)$$

$$r_s\,\Delta\kappa_j = +(\beta + z'')\sin\alpha \qquad (16b)$$

$$r_s\,\tau = -\beta' + z' \qquad (16c)$$

In addition to the change of the curvatures shown in the equations (16a,b), it is necessary to add the change of the curvatures which are based on the mounting of the piston

ring. (Change of curvature from the open or free shape condition to the closed condition)

$$r_s\ \Delta\kappa_r = k\left(1+\cos\varphi\right) \tag{17}$$

Where:
k is the piston ring factor [1,11]

$$r_s\ \Delta\kappa_i = -(\beta + z'')\cos\alpha + k\left(1+\cos\varphi\right)\sin\alpha \tag{18a}$$

$$r_s\ \Delta\kappa_j = +(\beta + z'')\sin\alpha + k\left(1+\cos\varphi\right)\cos\alpha \tag{18b}$$

$$r_s\ \tau = -\beta' + z' \tag{18c}$$

The elastic energy

The elastic energy, E, will be composed of the bending energy around the principal axis i, j and the torsion energy.

$$E = \int_{-\pi}^{+\pi} F(\beta,z)\, r_s\ d\varphi \tag{19a}$$

$$F(\beta,z) = \frac{1}{2} E\, J_i \left(\Delta\kappa_i\right)^2 + \frac{1}{2} E\, J_j \left(\Delta\kappa_j\right)^2 + \frac{1}{2} C\, \tau^2 \tag{19b}$$

Where:

E	is Young's modulus
$G = \frac{E}{2(1+\mu)} = \frac{E}{2.6}$	modulus of rigidity
J_i , J_j	principal moments of inertia
$C = G\, C_{tor}$	torsional rigidity
C_{tor}	torsion constant

Equations (18a,b,c) will be inserted in equation (19b).

$$F(\beta,z)\frac{2\, r_s^2}{E} = \left(J_i \cos^2\alpha + J_j \sin^2\alpha\right)(\beta + z'')^2 + \frac{C}{E}(-\beta' + z')^2 - 2\left(J_i - J_j\right)\sin\alpha\ \cos\alpha \times k\left(1+\cos\varphi\right)(\beta + z'') + \left(J_i \sin^2\alpha + J_j \cos^2\alpha\right) \times k^2\left(1+\cos\varphi\right)^2 \tag{20}$$

The last summand is constant after integration and is omitted from further consideration.
The principal moments of inertia
J_i and J_j are transformed by known formulas to the axis of the coordinate system (x,y).

$$I_{yy} = J_i \cos^2\alpha + J_j \sin^2\alpha \tag{21a}$$

$$I_{xy} = \left(J_j - J_i\right)\sin\alpha\cos\alpha \tag{21b}$$

Equation (20) is reduced to the following equation:

$$F(\beta,z)\frac{2\, r_s^2}{E} = I_{yy}(\beta + z'')^2 + \frac{C_{tor}}{2.6}(-\beta' + z')^2 - 2\, I_{xy}\ k\left(1+\cos\varphi\right)(\beta + z'') \tag{22}$$

If $M(\varphi)$ are the moments and $F(\varphi)$ the axial forces acting on the ring circumference (based on the circumferential unit of length) the variegate total energy is described by:

$$E = \int_{-\pi}^{+\pi} \begin{pmatrix} F(\beta,z) - M(\varphi)\,\beta \\ -F(\varphi)\, r_s\ z \end{pmatrix} r_s\ d\varphi \tag{23}$$

The equations of Euler

The necessary conditions for the minimum of equation (23) are the equations of Euler (24a,b).

$$I_{yy}\left(\beta+z''\right)+\frac{C_{tor}}{2.6}\left(-\beta+z\right)''=$$
$$M(\varphi)\frac{r_s^2}{E}+I_{xy}\,k\left(1+\cos\varphi\right) \qquad (24a)$$

$$I_{yy}\left(\beta+z''\right)''-\frac{C_{tor}}{2.6}\left(-\beta+z\right)''=$$
$$F(\varphi)\frac{r_s^3}{E}-I_{xy}\,k\cos\varphi \qquad (24b)$$

The piston ring gap ends are stress free because the values of the moments are zero. The results of this are the following boundary conditions:

$$\left(-\beta+z\right)'=0$$
$$\left(\beta+z''\right)=0$$
$$\left(\beta+z''\right)'=0 \qquad (25)$$
$$\text{for}\quad \varphi=-\pi \quad\text{and}\quad \varphi=\pi$$

New variables are introduced:

$$f_o(\varphi)=\frac{F(\varphi)}{I_{yy}}\frac{r_s^2}{E}$$
$$m_o(\varphi)=\frac{M(\varphi)}{I_{yy}}\frac{r_s^2}{E}=f_o(\varphi)\,x_o(\varphi) \qquad (26a\text{-}c)$$
$$p=\frac{C_{tor}}{2.6\,I_{yy}}$$

The variables are inserted in the equation (24a,b).

$$\left(\beta+z''\right)+p\left(-\beta+z\right)''=$$
$$m_o+\sum_{i=1}^{4}f_i\,x_i+\frac{I_{xy}}{I_{yy}}k\left(1+\cos\varphi\right) \qquad (27a)$$

$$\left(\beta+z''\right)''-p\left(-\beta+z\right)''=$$
$$f_o\,r_s+\sum_{i=1}^{4}f_i\,r_s-\frac{I_{xy}}{I_{yy}}k\cos\varphi \qquad (27b)$$

The variables $f_i(\varphi)$ describe the unknown reaction forces with the corresponding distances $x_i(\varphi)$ to the center of mass (Figure 4) . By using the 3 functions g_i (28a,b,c)

$$g_1(\varphi)=\sum_{i=0}^{4}f_i\left(r_s+x_i\right)$$
$$g_2(\varphi)=\sum_{i=0}^{4}f_i\,r_s \qquad (28a\text{-}c)$$
$$g_3(\varphi)=\sum_{i=0}^{4}f_i\,x_i$$

$$g_1(\varphi)=g_2(\varphi)+g_3(\varphi) \qquad (28d)$$

it is possible to describe equations (27a,b) as equations (29a,b).

$$\left(\beta+z''\right)+p\left(-\beta+z\right)''=$$
$$g_3(\varphi)+\frac{I_{xy}}{I_{yy}}k\left(1+\cos\varphi\right)$$
$$-\frac{I_{xx}}{I_{yy}}\frac{y_s}{r_s}k \qquad (29a)$$

$$\left(\beta+z''\right)''-p\left(-\beta+z\right)''=$$
$$g_2(\varphi)-\frac{I_{xy}}{I_{yy}}k\cos\varphi \qquad (29b)$$

The last summand of equation (29a) describes the reversing moments of the bending forces from mounting the piston ring with the lever arm y_S. The variable y_S describes the distance from the center of mass to the pivot point of the

running surface. Reversing moments occur especially for asymmetrically barreled or taper-faced rings.

Integration of Equations (29a,b) and the Balance

The equations (29a,b) describe the deformation of the loaded piston ring. These equations can be solved by partial integration under the condition of the equations (25). The results are described in the following equations:

$$\beta = \frac{1+p}{2p}\int_{-\pi}^{\varphi} g_1(t)\sin(\varphi - t)\,dt$$
$$-\frac{1+p}{2p}\int_{-\pi}^{\varphi} g_1(t)(\varphi - t)\cos(\varphi - t)\,dt$$
$$-\frac{1}{p}\int_{-\pi}^{\varphi} g_3(t)\sin(\varphi - t)\,dt$$
$$+\frac{I_{xy}}{I_{yy}}k\left(1+\frac{\varphi}{2}\sin\varphi\right)$$
$$-\frac{1+p}{p}\frac{I_{xx}}{I_{yy}}\frac{y_s}{r_s}k\left(\frac{\varphi}{2}\sin\varphi - \cos\varphi\right)$$
$$-\frac{I_{xx}}{I_{yy}}\frac{y_s}{r_s}k(1+\cos\varphi)$$
$$+A\cos\varphi + B\sin\varphi + C \qquad (30a)$$

$$z = \frac{1+p}{2p}\int_{-\pi}^{\varphi} g_1(t)\sin(\varphi - t)\,dt$$
$$-\frac{1+p}{2p}\int_{-\pi}^{\varphi} g_1(t)(\varphi - t)\cos(\varphi - t)\,dt$$
$$-\frac{1}{p}\int_{-\pi}^{\varphi} g_2(t)(\varphi - t)\,dt$$
$$+\frac{1}{p}\int_{-\pi}^{\varphi} g_2(t)\sin(\varphi - t)\,dt$$
$$+\frac{I_{xy}}{I_{yy}}k\frac{\varphi}{2}\sin\varphi$$
$$-\frac{1+p}{p}\frac{I_{xx}}{I_{yy}}\frac{y_s}{r_s}k\frac{\varphi}{2}\sin\varphi$$
$$+A\cos\varphi + B\sin\varphi + C \qquad (30b)$$

A, B and C are the integration constants. They are eliminated by using the conditions of balance.
The conditions of balance are:

$$\int_{-\pi}^{\pi} g_2\,d\varphi = 0$$
$$\int_{-\pi}^{\pi} g_1\sin\varphi\,d\varphi = 0 \qquad (31a\text{-}c)$$
$$\int_{-\pi}^{\pi} g_1\cos\varphi\,d\varphi = 0$$

If equations (30a,b) are inserted into equations (29a,b), equations (30a,b) can be verified.

The Reaction Forces

The deformations are limited by the piston ring groove height. According reaction forces appear which limit the deformations and force the ring into the groove. This contact problem in the software is solved by the help of the procedure of Wolfe, a modified simplex algorithm [4,7,8].
To calculate the complete piston environment at least 4 functions $f_i(\varphi)$ are necessary. Two at the top side and two at the bottom side of the piston ring. In conjunction with the functions $\beta(\varphi)$ and, $z(\varphi)$they describe the solution to the problem.

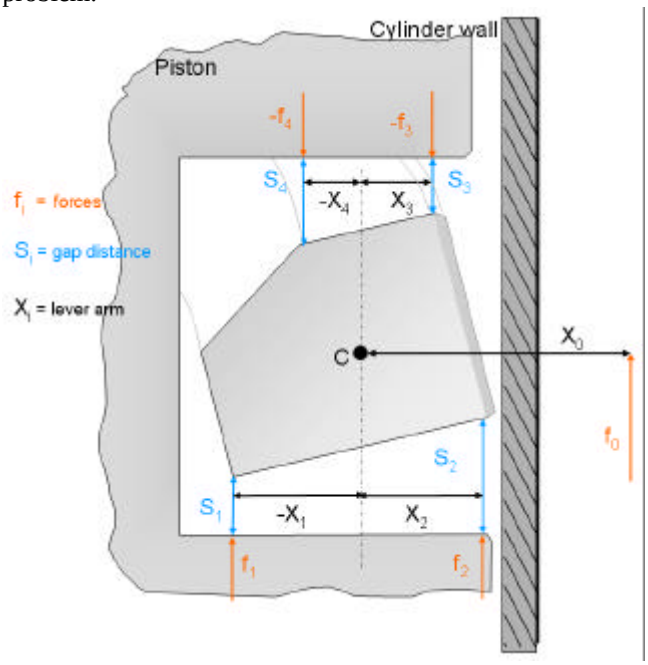

Figure 4 shows the resultant of the externally acting forces f_o and the resulting reaction forces f_i

The reaction forces act upon the levers x_i (Figure 4). f_o is the force and $f_o x_o$ is the moment. f_o and $f_o x_o$ act externally upon the piston ring. $f_i \ (i=1...4)$ are the reaction forces that balance the ring. $S_i \ (i=1...4)$ are the clearances between the ring and the groove. C is the center of mass from whose distance the levers x_i are measured.

$f_i \ (i=1...4)$ and $S_i \ (i=1...4)$ are alternative. Either $S_i \ (i=1...4)$ or $f_i \ (i=1...4)$ must be 0 at every point at the circumference.

That means that:

$$S_i(\varphi)\, f_i(\varphi) = 0 \quad (i=1...4) \qquad (32a)$$

The restrictions of the algebra signs are also significant:

$$S_i(\varphi) \geq 0 \quad (i=1...4)$$
$$f_i(\varphi) \geq 0 \quad (i=1...2) \qquad (32b)$$
$$f_i(\varphi) \leq 0 \quad (i=3...4)$$

If N is the axial clearance, it is possible to calculate the clearances with the help of the deformation of equation (30a,b).

$$S_i = (r_s\, z + x_i\, \beta) \quad (i=1...2)$$
bottom groove flank (33a)

$$S_i = N - (r_s\, z + x_i\, \beta) \quad (i=3...4)$$
top groove flank (33b)

Under the conditions of the algebra signs (32b), it is necessary to calculate 6 functions ß, z and $f_i \ (i=1...4)$. Therefore, 6 equations are available (30a,b) and the four equations of (32a).

Gas dynamics in the Clearances and in the Closed Gap of the Piston Ring

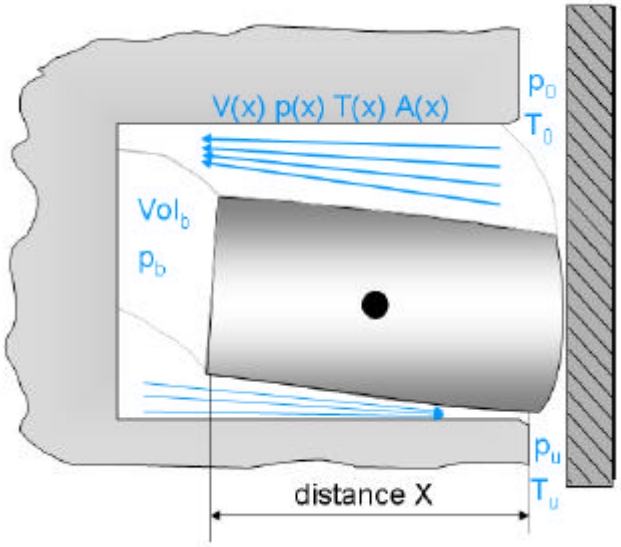

Figure 5 : The gas flow to and from the volume behind the ring

Figure 5 shows the gas flow between the piston and the piston ring top side and the piston ring bottom side respectively. The piston ring twists and the clearances are convergent. It is also possible that the clearances are divergent. This can happen, for example, if the twist angle is positive or during the ring movement.
The gas flow is activated by the pressure difference p_0 - p_b and p_b – p_u. By this process the chamber Vol_b behind the ring is filled or emptied. In summary, gas flows from the combustion chamber through the top clearances to the volume behind the ring and from there through the bottom clearances to the inter-ring volume. Part of the gas also flows directly through the gap ends to the inter-ring volume. This gas, flowing through the gap ends, which depends on the size of the closed gap, amounts to 30- 40 % of the total. It is also possible that the direction of the gas flow goes upward if the inter-ring pressure is higher then the combustion pressure ("blow-back").

The calculation of the gas flow and its pressure gradients, is fundamental for calculating the ring movement. It is not enough to calculate the flowing gas mass, it is absolutely essential to specify the state variable $p(x)$. This value is decisively responsible for the reaction forces, twist and arch of the piston ring. The gas flow mass in the clearance is constant, the gas pressure depends on its distance x. The ring position and the twist influence the clearance geometry and vice versa the clearance geometry influences the deformation of the piston ring.

Physical Properties and the Calculation of the Mach Number

The gas flow is described by the following physical conditions:

a) subsonic-flow.

b) In the clearance between the ring and the groove, the sound velocity cannot be exceeded. Therefore, no gas shocks are possible in the clearance. Due to the narrowness of the clearance in proportion to its length, the gas flow is highly restricted by friction. The gas molecules hit the ring side and the piston groove.

c) This leads to a heat exchange between the groove flanks and the gas flow. Therefore, the flow is neither isothermal nor adiabatic.

The equation of motion for gas under these conditions can be found in [5,6]. The problem c) is solved with the analogy of Reynolds, mentioned in [5].
The following differential equation for the Mach number is one of the important equations of motion from [5].

$$\frac{dM^2}{M^2} = -2\frac{1+\frac{k-1}{2}M^2}{1-M^2}\frac{dA}{A} + \left(1+kM^2\right)\frac{1+\frac{k-1}{2}M^2}{1-M^2}\frac{dT_S}{T_S} + kM^2\frac{1+\frac{k-1}{2}M^2}{1-M^2}4f\frac{dx}{D} \qquad (34)$$

M(x)	=V/c Mach Number
k = 1.4	ratio of specific heats
A (x)	cross-sectional area of the clearance
Ts (x)	stagnation temperature
f	coefficient of friction
	f depends on the Reynolds Number
D	mean hydraulic diameter

To solve the differential equation (34) a nummerical integration is necessary. In this case, a Runge-Kutta method with step control is advisable because M varies more as it approaches 1.
The gas flow mass w is constant inside the clearance length and can be calculated as:

$$w = \rho A V = k\frac{p}{c}AM \qquad (35)$$

ρ is the density

To start the calculation of (34), M has to be chosen so that the finished pressure $p_{end} = p_b$ at the clearance end will be reached. M_{start} has to be variated with the help of "regula falsi". The other input values at the beginning of the clearance are known, so that the constant w can be calculated with equation (35). It is also possible to calculate the pressure p(x) in the clearance with (35) as well the target value p_{end}.

Choked Flow by Friction

Depending on the pressure gradient, it is possible that the flow is choked by friction. Choked flow happens during the leakage of the gas at the clearance end if the gas has reached sound velocity in the clearance. It immediately expands to the pressure level p_b of the volume chamber. The excessive energy reacts by obelisk waves in the chamber outside of the clearance. The gas flow in the clearance is not influenced by this effect. By reason of the subsonic flow no choking can occur in the clearance.

The gas velocity can not be bigger than the sound velocity. It is necessary to find M_{start}, so that M inside the clearance reaches the maximum value and stays smaller then 1. At the end of the clearance a p_{limit} is fixed.
p_{limit} depends only on conditions at the start and not on p_b. p_{end} can not be smaller than p_{limit}. If $p_b < p_{limit}$ then the flow is choked and at the end of the clearance is:
$p_{end} = p_{limit}$.

In a choked flow and either convergent or straight clearance, M = 1 is reached at the end of the clearance. In divergent clearances M has its maximum close to the start of the clearance. The flow through the closed gap can be solved in the same way.

PART 3: MEASUREMENT AND SIMULATION

Concept of measurements of ring movement (CUMMINS)

Experimental Work

Cummins Engine Company carried out the experimental work. Information on part of this work was reported previously by Chen and Richardson [12].

Engine

The engine used for this work was

Engine Model: 1994 Cummins
C Engine Displacement: 8.3L
Rating: 186kW (250hp) at 2200rpm
Bore: 114mm diameter
Stroke: 135mm
Connecting Rod Length: 216mm

Instrumentation

Cylinder #5 was instrumented with ten (10) sensors shown in Table 1 and Figure 6. The sensors mounted on the piston used a grasshopper linkage system to bring out the measurements from the engine.

Table 1 List of Instrumentation

Channel #	Sensor Label	Description
Pressures Sensors		
01	CylPr	Cylinder Pressure
02	Liner	Liner Pressure
03	L3MA	Third Land Major Thrust Side
04	L2MA	Second Land Major Thrust Side
05	L2MI	Second Land Minor Thrust Side
Ring Motion Sensors		
06	R2MI	Second Ring Motion Sensor - Minor Thrust Side
07	R1MI	Top Ring Motion Sensor - Minor Thrust Side
08	R3MA	Oil Ring Motion Sensor - Major Thrust Side
09	R2MA	Second Ring Motion Sensor - Major Thrust Side
10	R1MA	Top Ring Motion Sensor - Major Thrust Side

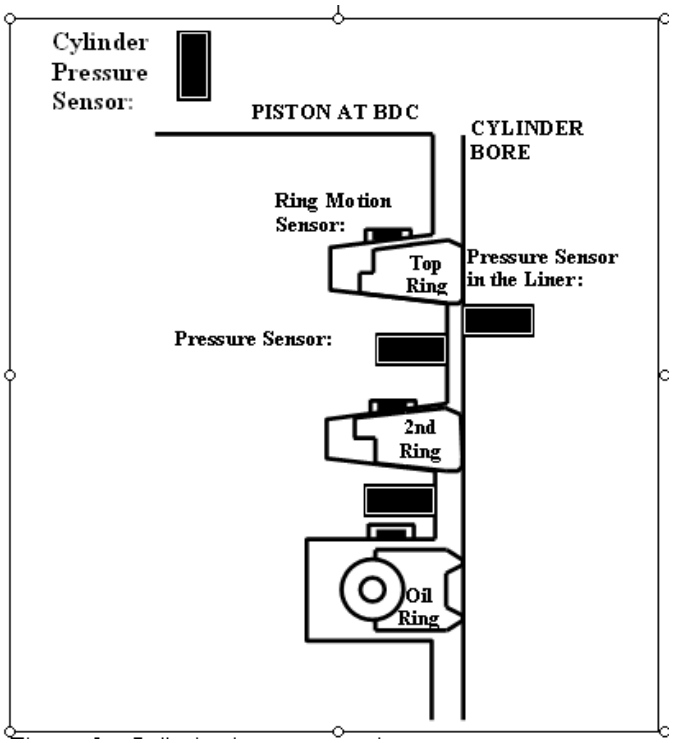

Figure 6 - Cylinder Instrumentation

The ring motion sensors were mounted on the top sides of the grooves to prevent a disruption of the sealing surface on the bottom side of the ring. It should be noted that the top ring motion sensor could overlap with the inter step in the top ring. The oil ring sensor was positioned in such a way that it could possibly overlap with the end of the ring. However, based on the measurements, the motion of the rings could clearly be seen.

The liner pressure sensor was mounted to be able to establish a reference of the inter-ring gas pressure. The sensor was placed in the liner at a position just below the top ring reversal at the bottom of the stroke. In this way the top ring never crossed the pressure sensor. It also allowed second land pressure measurements at Bottom Dead Center (BDC) witch was used for referencing the inter-ring gas pressure measurement.

When measurements were made, 100 individual consecutive cycles of data were stored per data point.

Measurement Results of One Condition Modeled

Figure 7 shows the measurement results from one condition (1600rpm, full load). The main characteristics of this measurement are that the top ring is shown to be fluttering. However, what is significant is that the fluttering is only seen on one side of the ring. The measurement on the thrust side of the piston shows the fluttering, the ring does not flutter on the anti-thrust side of the piston. This difference is not a function of the side of the piston as much as it is a

function of the location of the ring gap relative to the measurement location. This is described in detail in the following sections.

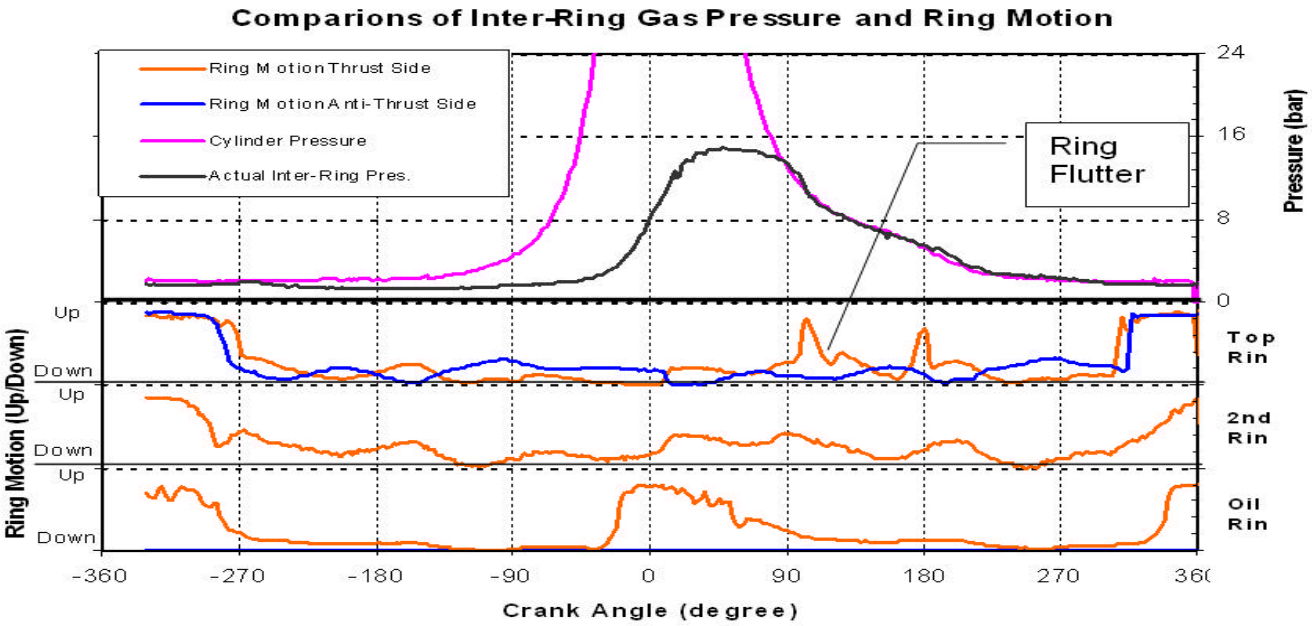

Figure 7 Measurement results

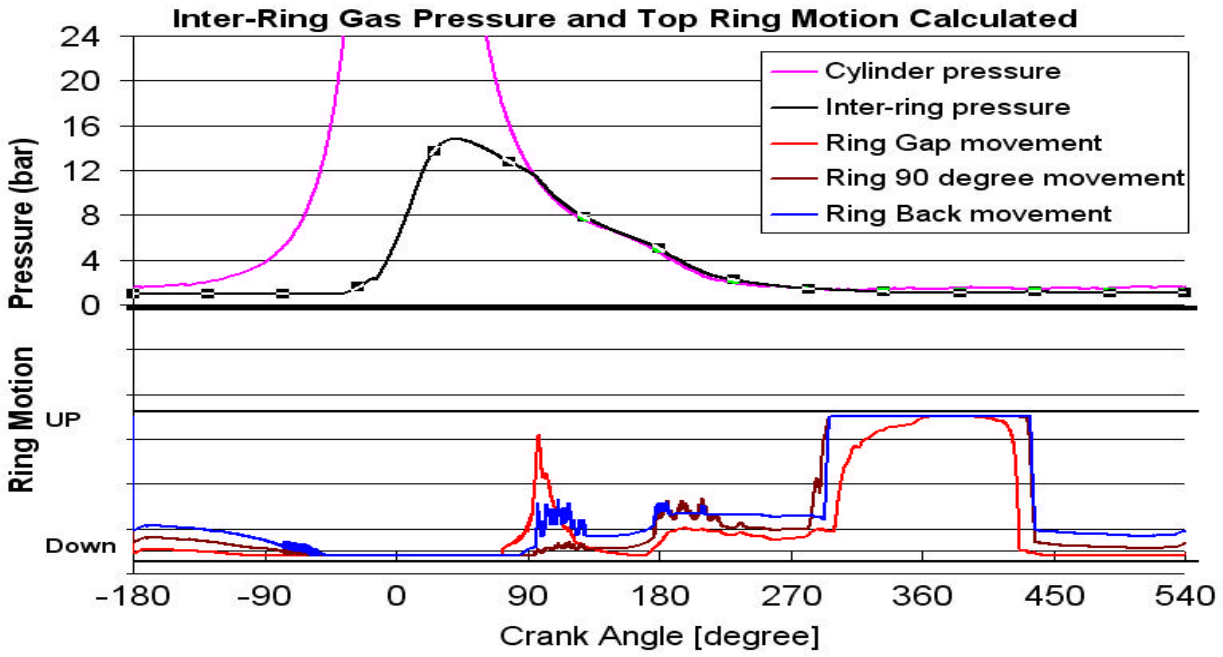

Figure 8: Simulation results of inter-ring pressure and top ring movement

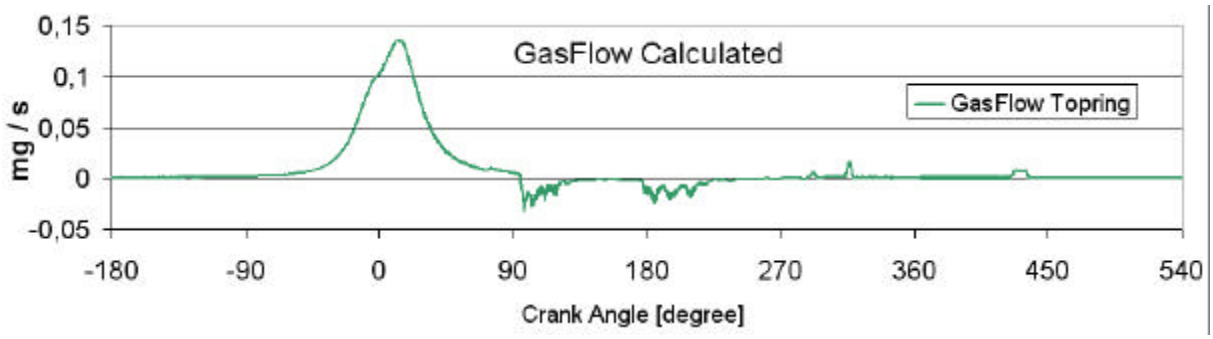

Figure 9: Simulation results of the Gasflow

Validation of Ring Movement and Blow-By by the Analytical Prediction Tool

As a reference, the Cummins test results were used to validate and understand the ring movement with its effects on blow-by. Based on the above mathematics a 3D tool was developed to investigate and understand the influence of design and engine kinematics on the engine performance. This full analytically solved tool takes into account the coupled conditions of the engine kinematics as well as the conditions of the mechanical components. The engine cycle is calculated in 0.5 degree steps, which achieves the optimized required accuracy. Figure 8 shows the coupled effects of different positions around the circumference. Due to the limited space of this paper it is not possible to show the complex results of a 3D calculation in a detailed way. However, the shown measured engine cycle is a perfect example, especially the top ring, to explain the result of the twist the gap ends are propped up with the inner edges (Figure 8). In this condition the ring can no longer prevent blow-by completely around the circumference. As shown in Figure 10 the piston ring, especially near the gap ends, is completely open for the gas flow through the groove.

In the next 20 degrees other areas around the circumference of the ring move upward by the change of (Fmas+ Ffriction) / Fgas. In this case a completely stabilized contact at the top side of the groove can not be achieved because the maximum mass force is not big enough to overcome the moments. Gas pressure differences are the main driver that forces the ring to start moving upward. However, when the ring lifts near the gap first, it opens a gas flow path around the ring which causes all the gas pressures to equalize around the ring. As a result, there is no longer any gas force pushing the ring upward anymore and the remaining forces and moments acting on the ring force the ring back down. This effect repeats itself causing the fluttering motion of the ring.

The twist and arching of the piston ring is caused by the moments acting on the rings, which can also occur in rectangular rings. If a ring does not lift uniformly around the ring all at once, the gas flow leak path is opened around the ring. As a result, the ring no longer seals the gases. In the example described above, when the ring lifts, the gases are blown upward (Figure 9). This may have an effect of reducing blow-by somewhat. However the “blow-back” may carry oil with it and adversely affect oil consumption. Also, as the ring twists and arches, it will affect the orientation of the running surface of the ring with respect to the liner. This may affect how well the ring scrapes oil.

A good understanding of how the forces act on the ring, how the ring moves in the groove and how the gases and oil flow past the ring is important for controlling oil consumption, blow-by and emissions.

fundamentals of ring movements in a visual form. The example of the fluttering situation shows the effects of ring movement being described in this paper.

The measured effect of ring fluttering is clearly visible when the inter-ring pressure equals the combustion pressure. The measurement result also show that the ring is not moving completely around its circumference to the top of the groove during the fluttering situation. The gap ends of the ring are already moving while the rest of the ring is still at the bottom flank. Because of this a gas flow path opens around the ring.
At around 90 degrees after combustion, the top ring starts moving as shown in Figure 2. The ring still has contact at the bottom groove side around the circumference while the gap ends are already moving to the top groove side. As a

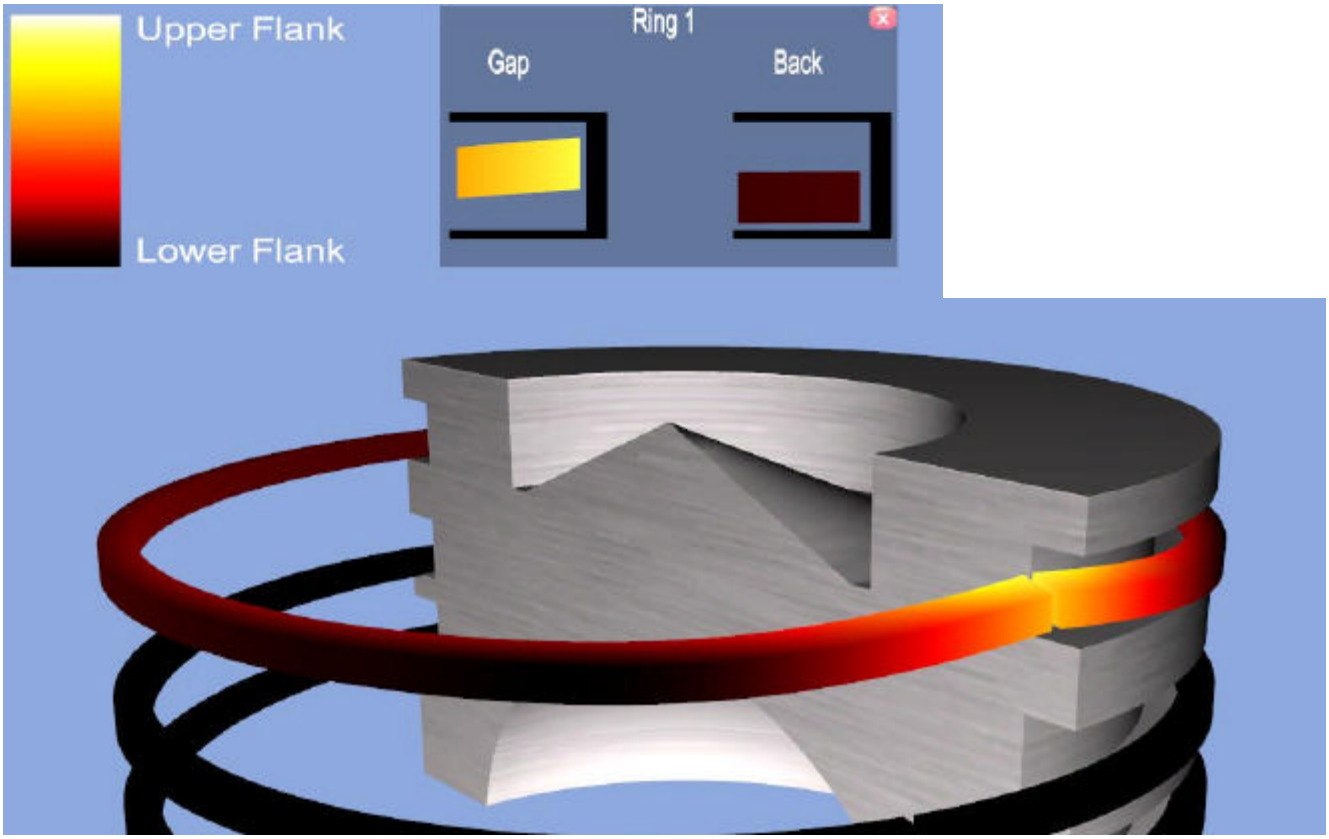

Figure 10: Visualization results of 3D top ring movement at 95 degrees crank angle

CONCLUSIONS

A physical description of the real ring and gas forces, as well as the effects of the moments during the engine cycle, is introduced to predict ring twist and movement. It is clearly apparent that the effects of ring movement and twist are much more instructive by theoretical inspection than by detailed engine measurements. To optimize the ring designs it is necessary to understand the fundamentals of the ring behavior under the different engine conditions. The simulations offer a clear indication of improvement potential. The high flexibility of the program contributes to rapid optimization in development projects.

NOMENCLATURE

a	wall thickness
φ	ring angle
$F(\varphi)$	axial force
$M(\varphi)$	moment
$f(\varphi)$	reduced axial force
$m(\varphi)$	reduced moment
$\beta(\varphi)$	twist angle
K	curvature
u , v	displacements
τ	torsion
s	arc length
r_S	distance from the center of mass to the cylinder center axis
$z(\varphi) \times r_S$	displacement in direction of the cylinder axis
E	Young´s modulus
G	modulus of rigidity
J_i , J_j	principal moments of inertia
I_{xx} , I_{yy} , I_{xy}	moments of inertia
C	torsional rigidity
C_{tor}	torsion constant
k	piston ring factor
A, B, C	integration constants
S	clearance between ring and groove
N	total clearance
$M(x)$	Mach Number
$p(x)$	gas pressure
k	ratio of specific heats
$A(x)$	cross-sectional area of the clearance
$T_S(x)$	stagnation temperature
f	coefficient of friction
D	mean hydraulic diameter
w	gas flow mass
ρ	density

REFERENCES

[1] C. Englisch, Kolbenringe, Springer-Verlag 1958

[2] A.E.H. Love, A Treatise on the Mathematical Theory of Elasticity, Cambridge University Press 1906

[3] K. Federhofer, Dynamik des Bogenträgers und des Kreisringes, Springer-Verlag, Wien 1950

[4] A. Mierbach, Berechnung der Radialdruckverteilung eines Kolbenringes, MTZ 55/2, 1994

[5] A. H. Shapiro, Compressible Fluid Flow, John Wiley & Sons, New York 1953

[6] H. Schlichting, Grenzschicht-Theorie, G. Braun, Karlsruhe 1965

[7] L. Collatz, W. Wetterling, Optimierungsaufgaben, Springer-Verlag 1966

[8] G. Hadley, Nonlinear and dynamic programming, Addision-Wesley Pub. Co,, 1964

[9] J. P. Corbat, Zur Mechanik der Kolbenringe mit unsymmetrischem Querschnitt, CIMAC 1975, Barcelona/Spanien

[10] A. Mierbach, Die Twistwinkel des L-förmigen Kolbenringes, MTZ 4/1975

[11] G. Dück, A. Mierbach, Piston Ring Manual, published by Goetze AG Germany

[12] Chen, Jinglei and Richardson, D.E., "Predicted and Measured Ring Pack Performance of a Diesel Engine," SAE Paper #2000-01-0918, 2000.

[13] Liang Liu, Tian Tian and Remi Rabute´ "Development and Applications of an Analytical Tool for Piston Ring Design," SAE Paper #2003-01-3112, 2003.